scientific reports

Check for updates

OPEN

EEG connectivity and BDNF correlates of fast motor learning in laparoscopic surgery

Ahmet Omurtag✉, Caroline Sunderland, Neil J. Mansfield & Zohreh Zakeri

This paper investigates the neural mechanisms underlying the early phase of motor learning in laparoscopic surgery training, using electroencephalography (EEG), brain-derived neurotrophic factor (BDNF) concentrations and subjective cognitive load recorded from $n = 31$ novice participants during laparoscopy training. Functional connectivity was quantified using inter-site phase clustering (ISPC) and subjective cognitive load was assessed using NASA-TLX scores. The study identified frequency-dependent connectivity patterns correlated with motor learning and BDNF expression. Gains in performance were associated with beta connectivity, particularly within prefrontal cortex and between visual and frontal areas, during task execution ($r = -0.73$), and were predicted by delta connectivity during the initial rest episode ($r = 0.83$). The study also found correlations between connectivity and BDNF, with distinct topographic patterns emphasizing left temporal and visuo-frontal links. By highlighting the shifts in functional connectivity during early motor learning associated with learning, and linking them to brain plasticity mediated by BDNF, the multimodal findings could inform the development of more effective training methods and tailored interventions involving practice and feedback.

Keywords Motor learning, Laparoscopic training, Functional connectivity, Brain-derived neurotrophic factor

Understanding the neural mechanisms responsible for motor learning is crucial for improving training and skill development, particularly in complex and high-stakes tasks such as laparoscopic surgery. Laparoscopic procedures require a unique set of psychomotor skills that must be developed through extensive practice, and training protocols may be optimised by identifying the brain activity patterns associated with learning. Laparoscopic novices must learn to generate new movements under the influence of unexpected forces which perturb the planned movements and altered haptic feedback from instruments[1]. In addition, they need to learn new perceptual-motor mappings involving the fulcrum effect and loss of depth perception[2], which measurably increase cognitive load[3]. In light of the benefits for patient safety and recovery and for health economics accruing from laparoscopy, a growing body of research has focussed on the physiological and neural correlates of the relevant skills[4–6] as well as on developing effective training strategies[7–11] including mindfulness[12] and neurofeedback interventions[13].

As anyone learning to play a musical piece can attest, initially effortful movements gradually become more automatic through practice, a widely appreciated feature of motor learning[14]. Learning new motor skills typically begin with large performance improvements, often within a single training session, as the brain encodes new movements in an internal model, acquired largely through error feedback[15,16]. The duration of fast learning can range from hours to weeks depending on the task[16]. In the fast phase of motor learning both cortico-cerebellar and cortico-striatal systems increase in the number and magnitude of functionally connected subareas[17]. Performance during this phase is cognitively and attentionally demanding, crucially recruiting the prefrontal (PFC) and parietal cortices[18,19], and can be disrupted by transcranial magnetic stimulation of the PFC[19].

The early phase is followed by a period of diminishing improvements as performance reaches a plateau and with prolonged practice a slow transition takes place toward automated skills resistant to interference while cognitive load continues to decline and multi-tasking ability steadily increases[20]. Fully automated motor performance primarily recruits the basal ganglia and associated cortical motor regions, as suggested by imaging studies[21] as well as animal electrophysiology[22] and computational modelling[23]. Automated performance may require less energy, according to the global neural efficiency hypothesis[17,18].

Neuroimaging studies have demonstrated that learning-induced plasticity in the human brain underlies visuomotor skill acquisition, which requires shifts in a distributed network of cortical and subcortical regions[24,25].

Nottingham Trent University, Nottingham, UK. ✉email: ahmet.omurtag@ntu.ac.uk

Synchrony in such networks plays a vital role in supporting visuomotor coordination, and can be detected in the form of phase coupling among band-limited signals from distinct neuronal populations[26–28]. This coordination of neuronal activity on a fine-temporal scale can be measured by leveraging methods which provide high temporal resolution, including electroencephalography (EEG)[29].

In this study we used EEG-based functional connectivity analysis to focus on the early phase of laparoscopy training. Connectivity was quantified by means of inter-site phase clustering (ISPC) (also called phase-locking value[30]). The skill acquired rapidly during the early phase of laparoscopic training lays the foundation for later consolidation, hence insights into its neural correlates are potentially useful for designing more targeted forms of practice and feedback.

We collected scalp EEG from novice participants as they performed in random order two laparoscopic training tasks of comparable difficulty – peg transfer and threading – with the first task repeated near the end of the session to assess the extent of performance increments. In addition, we measured BDNF levels from blood samples and subjective survey-based cognitive loads. BDNF is a protein that plays a crucial role in the brain's ability to reorganise and form new neural connections by facilitating synaptic plasticity and long-term potentiation, which are essential for learning and memory formation[31,32]. NASA-TLX scores were used to elucidate the cognitive demands imposed by the learning task.

The results demonstrated simultaneous improvement in speed and accuracy as well as reduction in cognitive load, and patterns of frequency-dependent connectivity were correlated with the extent of motor learning as well as BDNF expression. We also showed that graph-theoretic properties of the functional networks during rest as well as task performance could be used to discriminate between high- and low-learners. Our multimodal approach, combining neurophysiological, molecular, and cognitive measures, could offer a comprehensive understanding of the complex processes underlying the initial phases of motor learning.

Results

Thirty-eight healthy adult volunteers without prior experience in laparoscopic surgery performed two types of laparoscopic training tasks on a laparoscopic simulator (Fig. 1A). After exclusions due to technical and other issues, the data from $N = 31$ participants were retained for further analysis (17 females, 14 males, age 21.61 ± 2.12 years). Their age range aligned with the typical age of medical trainees who begin learning laparoscopic skills. Each participant initially performed a reaction task (T0) and the initial 2-minute rest (R1). Next they executed the first training task (T1) selected randomly from the two types of tasks, a rest episode (R2), followed by the other task (T2), another rest (R3), the repeated performance of the first task (T1R) and the last rest episode (R4) (Fig. 1B). EEG was recorded throughout the experiment from 19 channels positioned at the standard 10–20 sites and performance and self-reported cognitive load were measured.

We first investigated the changes in participants' behavioural and subjective metrics (Fig. 1C-F). Then their functional connectivity across Rest and Task episodes was calculated at multiple frequencies and ranges of

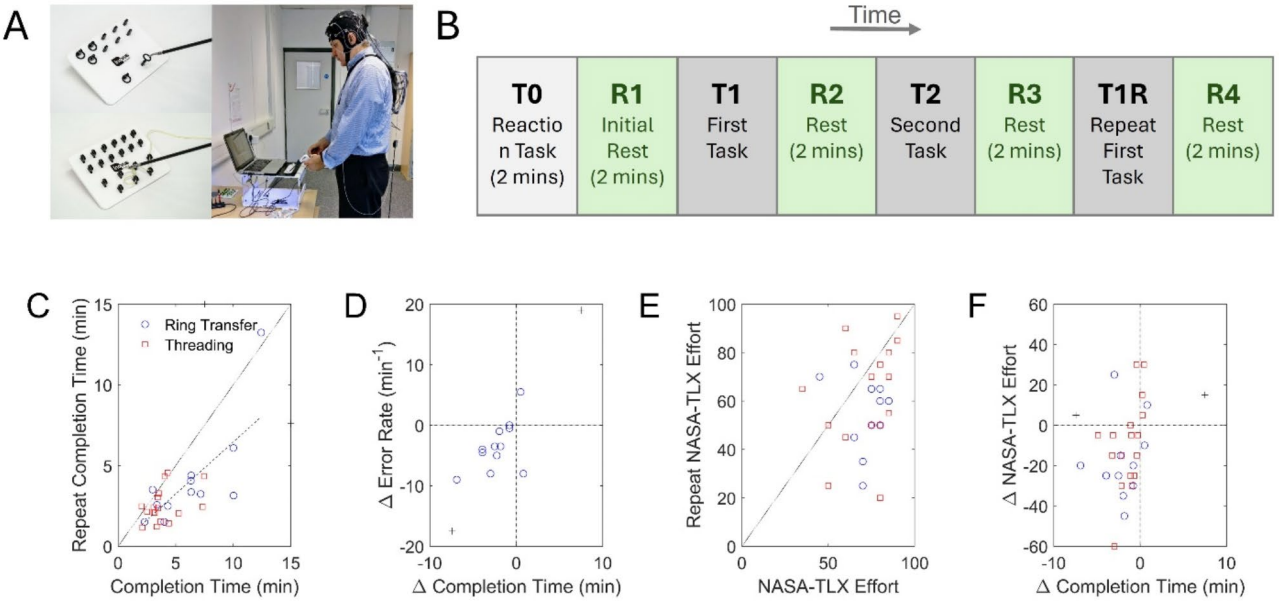

Fig. 1. Experiments and behavioural and subjective indicators of learning. (**A**) Photograph of Ring Transfer and Threading boards and a task performing participant. (**B**) Experimental procedure. (**C**) Completion times of initial (x-axis) and repeat (y-axis) performances of the Ring transfer (blue circles) and Threading (red squares) tasks. (**D**) Change in (repeated minus initial) Error Rate v change in Completion Time for the Ring Transfer task. Threading errors were not tracked. (**E**) NASA-TLX Effort score for the initial (x-axis) and repeated (y-axis) tasks. (**F**) Change in NASA-TLX Effort score v change in Completion Time. Results from the two subjects who reached the 15 min max allowed time in the ring task are indicated by a black plus sign.

cortical distance (Fig. 2). On this basis, we studied the association between motor learning, BDNF expression, and functional connectivity (Figs. 3 and 4) and that between motor learning and network integration and segregation properties (Fig. 5; Table 1).

Behavioural and subjective measures of fast motor learning

Figure 1C shows the task completion times in the repeated performance (T1R) as a function of the completion times of the same task in the initial performance (T1). Data from most participants, represented by small circles in the figure, were below the diagonal (dotted) line indicating that the completion times had decreased. Fitts' law for reaching movements predicts that in the absence of learning increases in speed may occur at the expense of accuracy[33]. To investigate whether this was the case we examined the dependence of the improvement in completion time (T1R minus T1) on the change in the rate of errors committed during task execution. The results (Fig. 1D) showed that for most participants the completion time and error rate had both decreased ($r = 0.89$, $p < 0.05$), suggesting that the relevant skills were acquired.

In order to investigate changes in cognitive load we examined the scatter plot of the Effort scores reported by each participant in the repeated and initial tasks (Fig. 1E). The plot showed that there were more data points

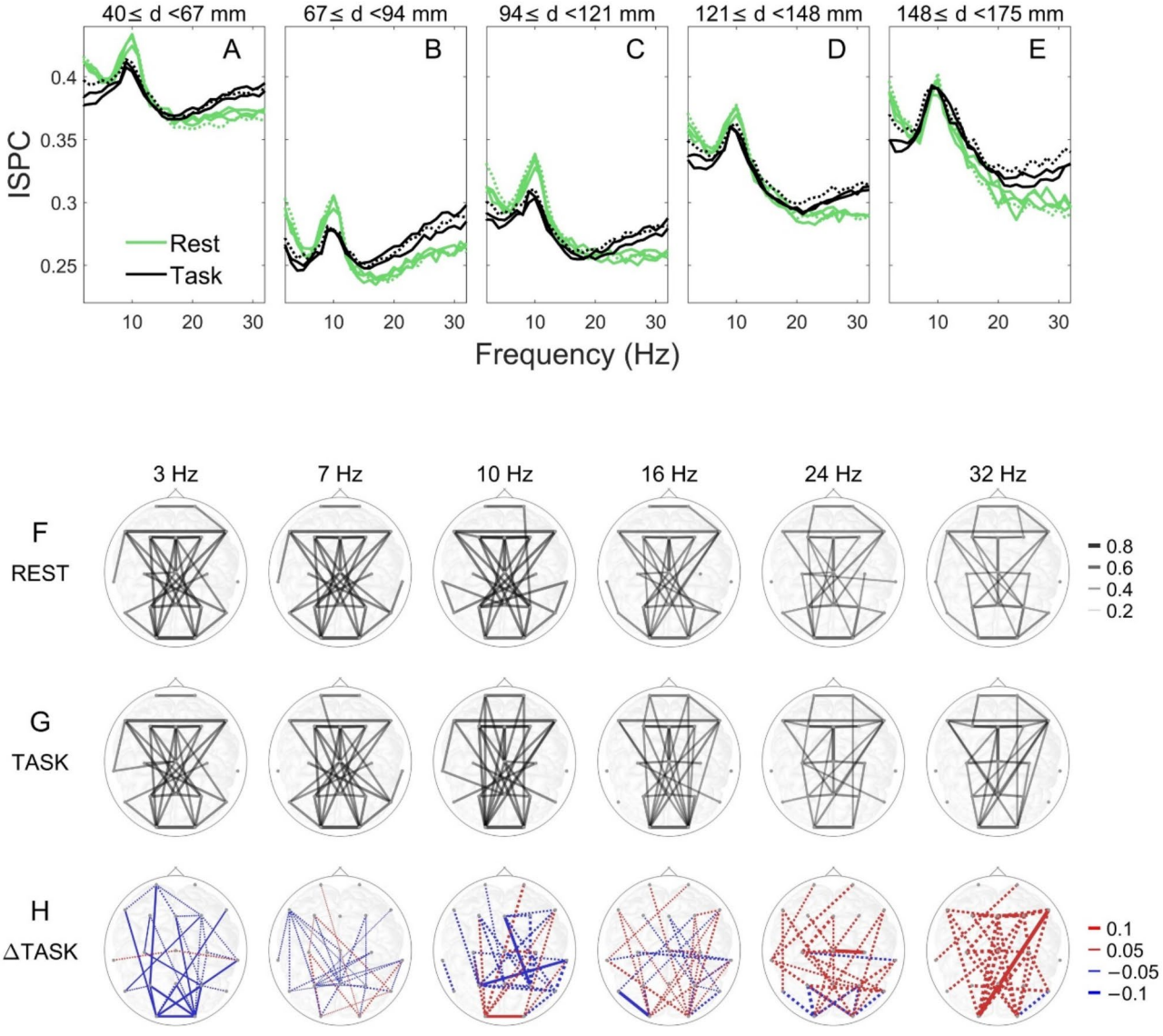

Fig. 2. Subject averaged functional connectivity during Rest and Task episodes. The top row shows the ISPC averaged across connections linking (**A**) short, (**B**–**D**) intermediate, and (**E**) long cortical distances as a function of the connection frequency, for the Rest (green curves) and Task (black solid) and T1R (black dotted) episodes. The range of cortical distance for each of these groups is indicated above each subplot. Also shown are ISPC for selected frequencies during initial Rest (**F**) and initial Task (**G**) episodes with the frequencies indicated above each column. The task-evoked change (Task minus Rest) in ISPC is shown in the bottom row (**H**) where increase and decrease are indicated by red and blue lines, respectively. The top 30 connections with the largest differences are shown.

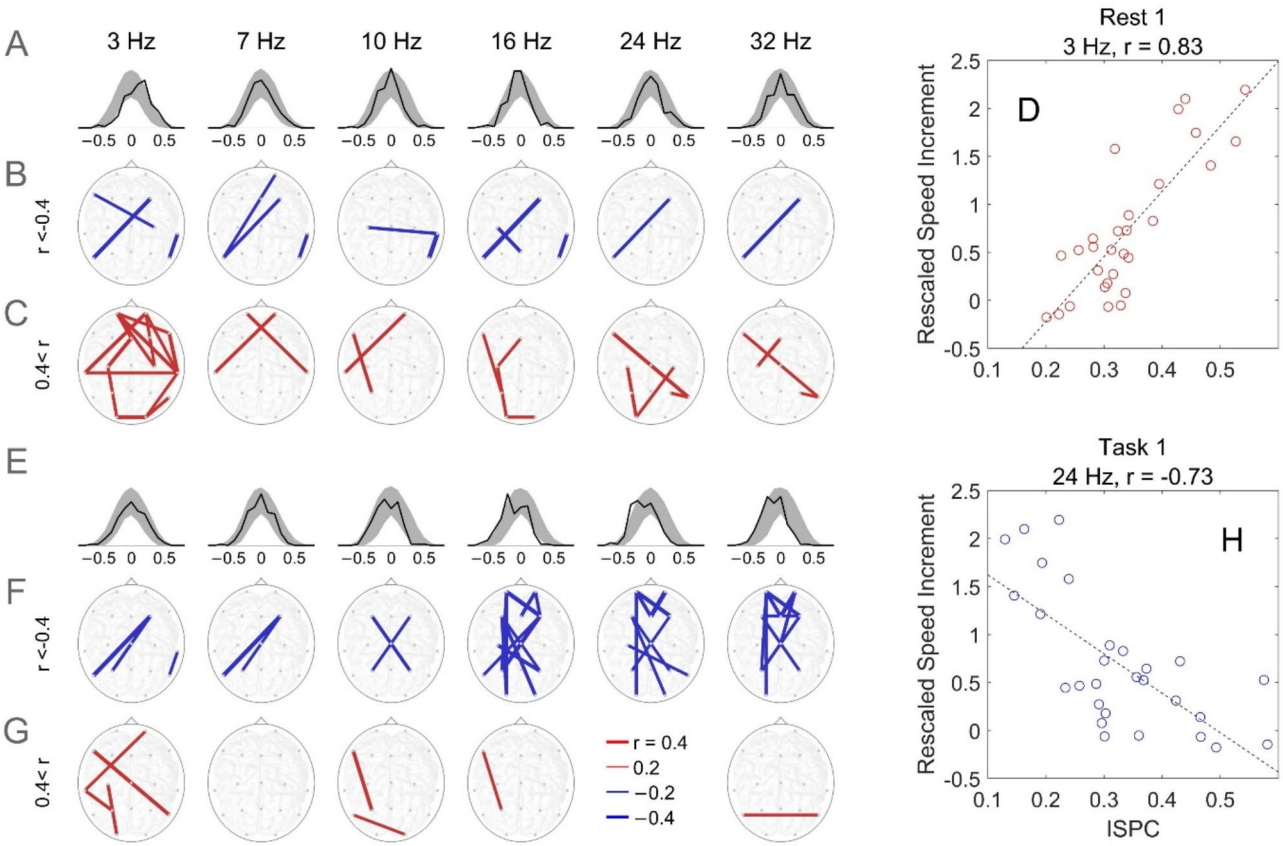

Fig. 3. The association between functional connectivity and performance improvement, quantified by the Pearson correlation between ISPC and Rescaled Speed Increment. ISPC was calculated during initial rest (**A**–**D**) and initial task performance (**E**–**H**). Histograms of correlation coefficients for the frequencies are displayed for rest (**A**) and task (**E**), with 95% confidence intervals indicated by grey shaded regions. Topographic illustrations are provided for the connections during rest (**B**) and during task (**F**) that were strongly anticorrelated ($r < -0.4$) with RSI; and during rest (**C**) and task (**G**) that were strongly positively correlated ($r > 0.4$) with RSI. Also shown are scatter plots of ISPC v RSI, where ISPC was calculated as the average of connectivity (**D**) at 3 Hz during rest and (**H**) at 24 Hz during task.

below than above the diagonal, hence there was an overall decrease in cognitive load. But this shift was less pronounced than in the behavioural metrics. The other dimensions of cognitive load and the average score had similar downward shifts, albeit lower in magnitude. We also investigated whether the decrease in completion time that was observed in the repeat task execution could have come at the expense of higher cognitive load. Figure 1F, which shows the scatter plot of increments in the reported Effort scores v the increments in completion times, suggests that most of the participants who performed the repeated task faster also experienced lower cognitive load, also suggesting the presence of fast learning ($r = 0.26$ (Ring), 0.45 (Threading)). Concurrent shifts in completion times, error rates, and cognitive load are illustrated in Figure S1.

Functional connectivity

Connectivity was quantified by ISPC to show the extent of clustering in the polar space of the phase angle differences between pairs of narrowly band-limited signals[34]. There were a total of 5472 distinct ISPC values as each ISPC was associated with a 1 Hz wide frequency band (in the range 1–32 Hz) as well as a specific pair of electrodes (with 171 undirected pairs of 19 electrodes).

To determine the dependence of ISPC on cortical distance we used the Montreal Neurological Institute (MNI) coordinates of the primary neuronal populations in the adult brain for the EEG electrodes, to associate an average distance with each electrode pair[35]. The pairs were grouped into short (40–67 mm), intermediate (67–94), (94–121), (121–148), and long (148–175 mm) range connections, where the means of the subject-averaged ISPC within each range were computed. Overall connectivity strength locally peaked around 10 Hz and the strongest connectivity was found over the shortest and longest distances (Fig. 2A-E). In all but the longest distances, the effect of task performance (Task (black curves) relative to Rest (green)) was to lower ISPC in the alpha and lower frequency ranges, while strengthening beta frequency links across all cortical distances.

We also examined the topographic locations of the strongest connections during Rest and Task performance. Figure 2F, G represent ISPC values by a line connecting a pair of sites. These links show the connections with the highest values of ISPC (only top 30 were selected to avoid clutter in the figure). Symmetric inter-hemispheric

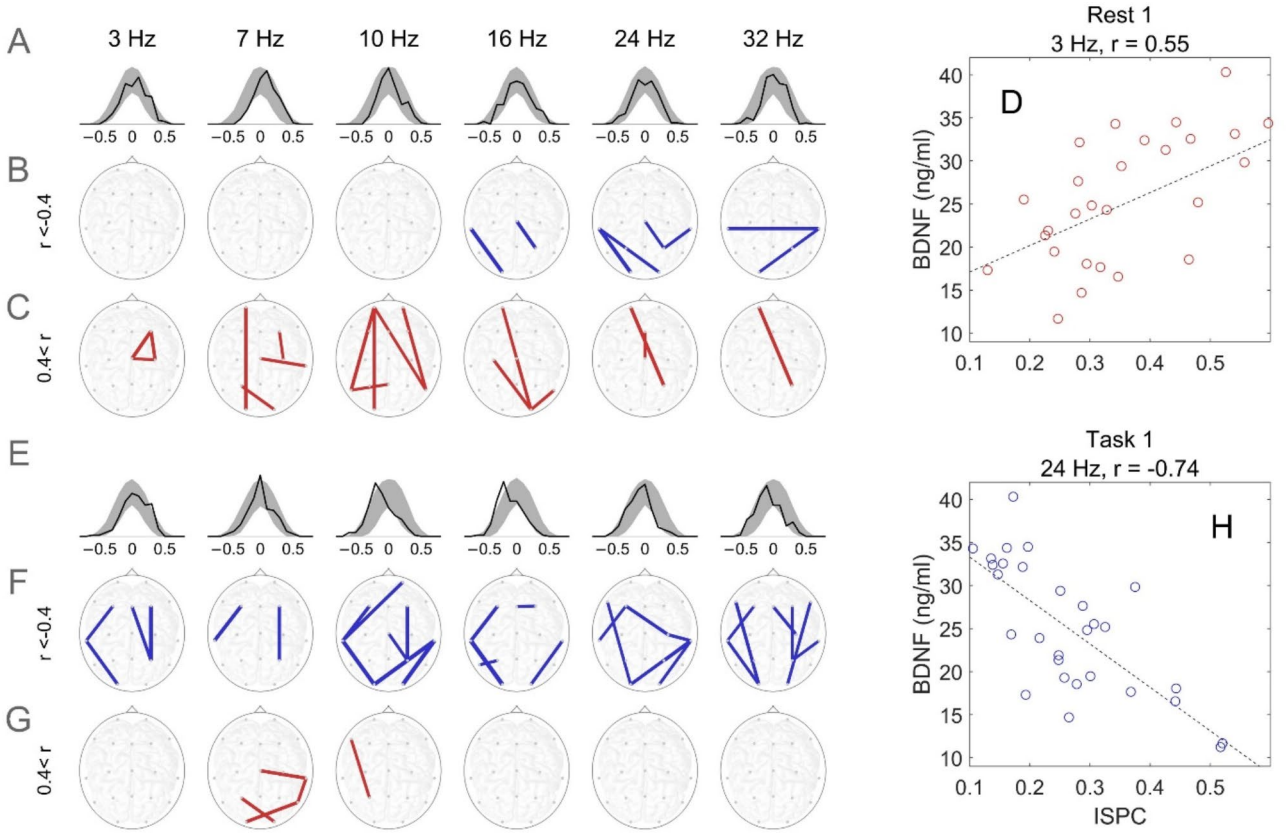

Fig. 4. The association between functional connectivity and BDNF. ISPC was calculated during initial rest (**A**–**D**) and initial task performance (**E**–**H**). Histograms of correlation coefficients for the frequencies are displayed for rest (**A**) and task (**E**), with 95% confidence intervals indicated by grey shaded regions. Topographic illustrations are provided for the connections during rest (**B**) and during task (**F**) that were strongly anticorrelated ($r<-0.4$) with BDNF; and during rest (**C**) and task (**G**) that were strongly positively correlated ($r>0.4$) with BDNF. Also shown are scatter plots of ISPC v BDNF, where ISPC was calculated as the average of connectivity (**D**) at 7 Hz during rest and (**H**) at 16 Hz during task.

frontal connectivity (F7-F8), as well as longitudinal inter-hemispheric connections (e.g. O1-F8 and O2-F7), particularly in the delta, theta and alpha frequencies were salient in both the initial rest (F) and the task (G). In addition intra-prefrontal connections (e.g. FP2-F8) appear in the beta frequencies.

The differences between ISPC under task and rest are brought out more clearly in Fig. 2H that shows the links with the largest differences between task (G) and rest (F). The line thickness is proportional to the magnitude of the difference. The figure indicates that at 10 Hz the task-evoked decreases occur mostly in the central areas in links that are short and medium distance, in agreement with Fig. 2A-C. The frequencies 3, 7, 10, 16, 24, and 32 Hz corresponding to the frequency ranges named delta, theta, alpha, and the low to high beta bands were selected for plotting connectivity in Fig. 2F-H. The task evoked changes in connectivity in Fig. 2H show increases in the high-beta bands in the bilateral occipital-frontal links as well as across the inter-hemispheric motor areas. The values of the ISPC in this figure are provided in Tables S1 and S2. Connections exceeding significance threshold ($p<0.05$, false discovery rate (FDR) corrected, see Materials and Methods) are shown by solid lines and the remaining ones by dotted lines.

Functional connectivity, motor learning and BDNF

Task execution speed (in units of tasks per minute) is the reciprocal of the task completion time. For the remainder of this analysis we have utilised speed as the performance metric, as higher speed directly indicates higher performance. But we first formulated a metric to quantify the extent of learning. Results had shown that increases in speed (ΔS) depended on the participants' initial speeds, such that individuals with a lower speed S_{T1} showed larger gains upon repeating the task (dashed line in Fig. 1A). Thus performance gains were dependent on the baseline performance. To minimise this confound we normalised the speed increment by the initial speed to obtain $\Delta S/S$, the Rescaled Speed Increment (RSI). We adopted RSI as the index of motor learning, to quantify the amount of learning regardless of the baseline laparoscopic performance. The latter may depend on such factors as visuomotor aptitude and video gaming experience[36,37] which were not our focus in this study.

Figure 3 shows the dependence of motor learning on connectivity during the initial rest (A-D) and initial task (E-H) episodes. The thickness of lines in the topographic plots (Fig. 3B-C and F-G) is proportional to

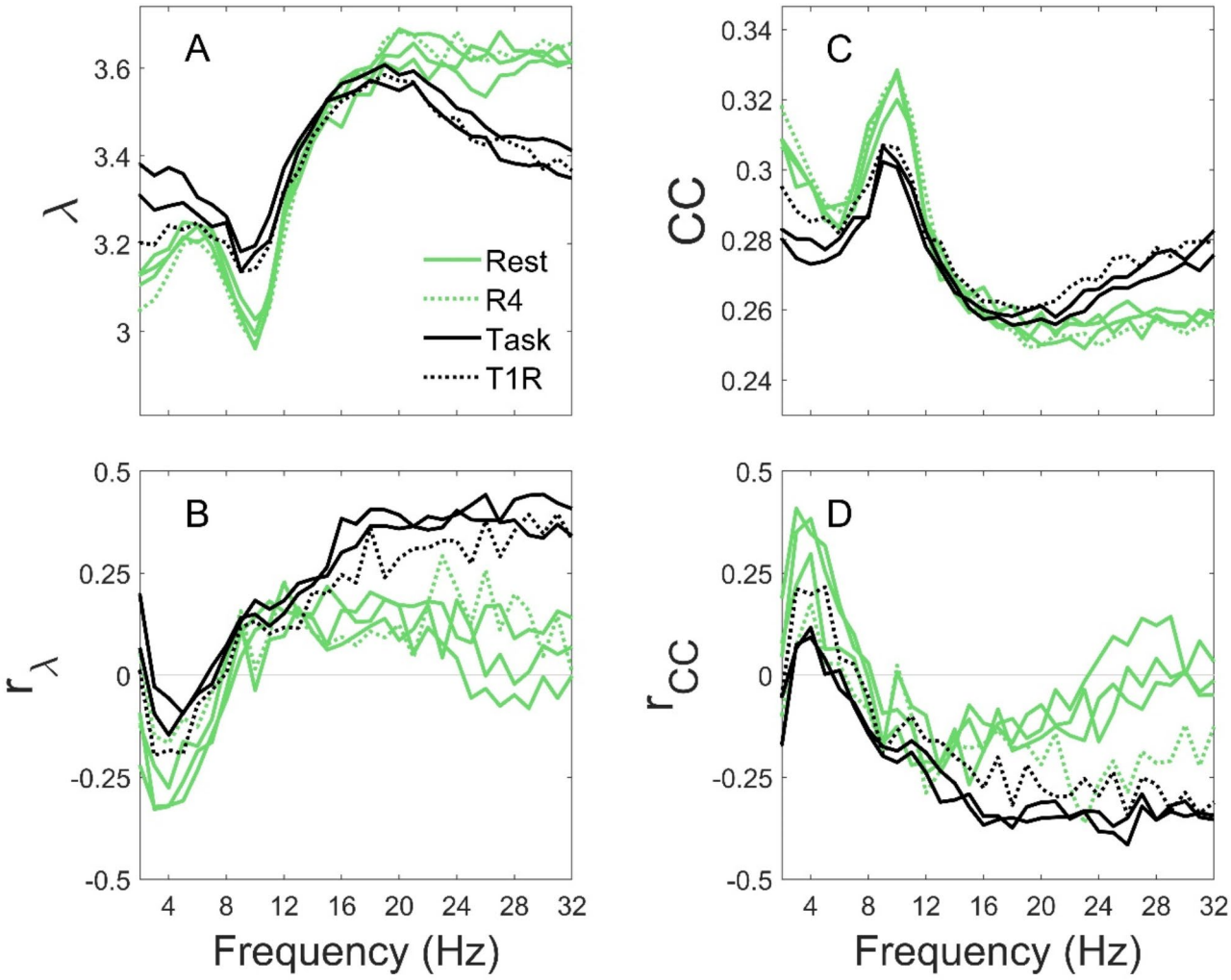

Fig. 5. Graph theoretic quantities and their association with motor learning quantified by RSI. Characteristic Path Length (**A**) and Clustering Coefficient (**C**) and the correlation between the Rescaled Speed Increment and Characteristic Path Length (**B**) and Clustering Coefficient (**D**) shown as functions of frequency, for Rest (green curves) and Task (black) episodes. The final Rest or Task episodes are indicated by dotted lines.

the magnitude of the Pearson correlation coefficients while the red and blue colours signify correlation and anticorrelation, respectively. Each column is for a selected frequency (shown at the top) while the connections whose correlation coefficients are within the distinct ranges have been segregated into separate rows for better visibility.

The histograms of the Pearson correlation coefficients for the rest episode remain within the 95% confidence interval (shaded regions in Fig. 3A) for most frequencies. However near 3 Hz, the histogram is skewed toward positive values. Figure 3B and C show all of the connections with the strongest negative (r<-0.4, blue lines) and positive correlations (r>0.4, red), respectively. This strongest correlations were selected for illustration purposes; the full range of correlations are included in Figure S2. There are more positive than negative correlations at this frequency, confirming the asymmetry in the histogram. Most of the strong positive connections were made by the frontal and temporal areas, with the frontopolar and right temporal sites emerging as hub-like regions. These connections correlated with motor learning (Table S1). The correlation coefficient for RSI and the average of all the ISPCs of the 3 Hz connections (red lines in the leftmost column of Fig. 3C) was 0.83, $p<0.05$. This strong correlation is evident in the scatter plot in Fig. 3D where each participant is represented by a red circle. The ISPC for each participant in this figure was calculated by averaging the ISPCs corresponding to the red lines in the 3 Hz topographic subplot C.

During task performance, on the other hand, the histograms of the correlation coefficients between RSI and ISPC, shown in Fig. 3E, indicate that the strongest predictors of motor learning were connections in the beta range. These were primarily frontal and frontoparietal and visuo-frontal, with coefficients in the range − 0.62 to − 0.40 (Table S2). Accordingly the histograms in this range, particularly at 24 Hz, are skewed toward the left. The scatter plot of RSI v ISPC at 24 Hz for the ISPC averaged over this group of connections ($r=-0.73$, $p<0.05$) is shown in subplot H. Although all correlations shown in the figure were significant at the 0.05 level, they were not significant after correcting for multiple comparisons using the FDR method.

Freq (Hz)	Path length			Clustering coefficient		
	Value	Correlation with RSI		Value	Correlation with RSI	
Rest 1						
3	3.17 ± 0.36	− 0.32	(− 0.62, 0.05)	0.30 ± 0.04	0.41*	(0.05, 0.67)
7	3.23 ± 0.40	− 0.15	(− 0.49, 0.23)	0.29 ± 0.05	0.07	(− 0.31, 0.42)
10	3.03 ± 0.39	0.11	(− 0.27, 0.46)	0.32 ± 0.06	− 0.08	(− 0.44, 0.29)
16	3.57 ± 0.49	0.17	(− 0.21, 0.51)	0.26 ± 0.04	− 0.19	(− 0.52, 0.19)
24	3.64 ± 0.52	0.04	(− 0.33, 0.40)	0.25 ± 0.05	0.04	(− 0.33, 0.40)
32	3.61 ± 0.59	0	(− 0.37, 0.37)	0.26 ± 0.06	0.03	(− 0.34, 0.39)
Task 1						
3	3.36 ± 0.43	− 0.03	(− 0.39, 0.34)	0.27 ± 0.04	0.07	(− 0.30, 0.43)
7	3.29 ± 0.41	0.02	(− 0.35, 0.38)	0.28 ± 0.05	− 0.07	(− 0.42, 0.31)
10	3.20 ± 0.49	0.15	(− 0.23, 0.49)	0.30 ± 0.06	− 0.19	(− 0.52, 0.19)
16	3.54 ± 0.48	0.38*	(0.02, 0.66)	0.26 ± 0.05	− 0.37	(− 0.65, − 0.00)
24	3.47 ± 0.44	0.40*	(0.04, 0.67)	0.27 ± 0.05	− 0.33	(− 0.62, 0.04)
32	3.35 ± 0.46	0.41*	(0.05, 0.67)	0.28 ± 0.06	− 0.34	(− 0.63, 0.03)

Table 1. Graph theoretic characterisation of functional networks and their association with motor learning. Subject averaged characteristic path length and clustering coefficient and their correlation with Rescaled Speed Increment for selected frequencies are shown for the initial Rest (R1) and initial Task (T1) episodes (*$p < 0.05$). The 95% confidence interval of the correlation coefficient is indicated in parentheses.

Figure 4 indicates the dependence of the correlation between ISPS and BDNF concentration on frequency for pre-task rest (A-C) and during initial task (E-G). We used the BDNF measured immediately after the completion of the initial task. The figure indicates that downregulation of the left temporal region's links with both occipital and frontal areas promoted BDNF production particularly in the alpha frequency range (F). In addition, intra-hemispheric connectivity between occipital and frontal areas in the high beta range were anti-correlated with BDNF. The scatter plots on the right exemplify the relationship between BDNF and the average of the ISPCs in particular frequency ranges. The resting ISPCs (red lines in the 7 Hz column of Fig. 3C) had $r = 0.65$, $p < 0.05$ and task-related ISPCs (blue lines in the 16 Hz column in Fig. 3F) had $r = -0.73$, $p < 0.05$ (uncorrected for multiple comparisons). The correlations between RSI and BDNF measured at any point during the experiment, with or without baseline correction, were small and not statistically significant (Table S3).

Network properties

By using ISPC as the weights of edges between nodes represented by electrodes, we constructed weighted undirected graphs whose properties provided descriptions of the overall connectivity profile and its association with motor learning. For these graphs we calculated the characteristic path length (λ) and clustering coefficient (CC). The reciprocal of λ quantifies network integration or the efficiency of information transfer across the network, while CC measures network segregation resulting from the extent to which nodes tend to cluster together.

We first investigated how network integration and segregation varied as a function of frequency. Figure 5A shows that in the beta frequency range (particularly for > 20 Hz) task performance resulted in a significant downward shift in λ (black curves), increasing the level of network integration relative to resting (green). By contrast task execution was associated with increases in λ around 10 Hz as well as in the lower frequency networks. Figure 5C shows that the task-evoked changes in CC were largely opposite to those in λ.

Figure 5B, D indicate that resting graph properties in the delta frequency range were strongly associated with motor learning, with peaks of $r_{\lambda} = -0.32$ and $r_{CC} = 0.41$ (3 Hz in Table 1). For task-related graph properties, the strongest predictors of learning were found broadly in the beta frequency range, particularly > 20 Hz, as shown by the black curves in Fig. 5B and D. Table 1 indicates that at the high end of the beta range, $r_{\lambda} = 0.41$ and $r_{CC} = -0.34$. Therefore over this frequency range lower functional connectivity across long (thus higher λ) as well as shorter cortical distances (thus lower CC) both appeared to promote motor learning.

Discussion

In this study novice participants performed laparoscopic surgery training tasks while their behavioural, subjective and neural measures as well as blood BDNF concentration were recorded. Participants showed significant gains in speed and accuracy when repeating a task, accompanied by small declines in cognitive load (Fig. 1). We identified task-evoked enhancements in high frequency functional connections, particularly those linking visual to frontal areas (Fig. 2). In addition, gains in performance were correlated primarily with beta connectivity during task execution ($r = -0.73$) and delta connectivity during the initial rest episode ($r = 0.83$) (Fig. 3). Connectivity was also correlated with BDNF with a bias toward anti-correlation in alpha and beta frequencies, but with a different topographic pattern that emphasised left temporal and visuo-frontal links (Fig. 4). Corresponding task-evoked changes and correlations with learning were observed for network characteristic path length and clustering, albeit with lower correlation coefficients (Fig. 5).

This study presents several novel findings. Firstly, it demonstrates and quantifies within-session learning in laparoscopic surgery training using the Rescaled Speed Increment, which is independent of the participants' baseline performance, providing a robust metric to assess skill acquisition during training sessions. Secondly, we utilised narrow-band inter-site phase clustering, rather than connectivity measures in the traditional wider frequency bands, to quantify the functional connectivity between different brain regions in the participants. Finally, and most significantly, the study has shown that shifts in brain's functional connectivity in specific combinations of frequency and topography were linked to performance enhancements as well as blood BDNF concentrations. In particular, the down-regulation of prefrontal and frontal connectivity was revealed to be a significant promoter of fast motor learning.

The earliest stages of sensorimotor learning are marked by rapid performance improvement and the expansion of neural representation of the skill in the brain[38,39]. To assess fast learning in our study, we concurrently tracked changes in both speed and the error rate. This allowed us to rule out the possibility of misinterpreting speed increases as learning, when they may have simply reflected movement along an unchanged speed-accuracy curve. Interestingly, participants who started with stronger baseline abilities showed smaller performance gains, potentially indicating that high performers may be near a performance plateau (Fig. 1C-D). In contrast, the shifts in cognitive load did not seem strongly tied to initial cognitive load levels (Fig. 1E-F), suggesting that cognitive load was not close to levelling off, consistent with the longer time-course of the automation process.

We found that ISPC was highest for the shortest and the longest distance connections with a noticeable trough in the intermediate distances (Fig. 2A-E). The distribution of axons in the brain is dominated by small-calibre, short-range connections together with a small number of very long, large-diameter fibres[40]. Since anatomical networks constrain functional ones[29] this may explain the U-shaped dependence of ISPC on cortical distance in the figure. It is also worth noting that if the phase clustering had been driven primarily by volume conduction, ISPC would have shown a steady decline with increasing cortical distance, rather than the observed non-monotonic dependence.

In Fig. 2A-E, task execution drives increases in connectivity over beta and decreases in the delta ranges. The fact that these shifts occur in similar ways across all cortical distances may be associated with brain's property of preserving inter-area cooperation independently of physical distance[41]. The figure also indicates that task execution lowers alpha ISPC, except for the longest distance connections. Alpha oscillations are closely linked to the default mode network (DMN) known to bilaterally span a set of areas from the frontal to the parietal, and can be upregulated by stimulating the alpha rhythm[42]. Therefore the blue lines in Fig. 2H over the frontal and parietal areas at 10 Hz are likely indicative of the task relevant down-regulation of the DMN.

The performance of bimanual visuomotor training tasks was expected to strengthen the high-frequency inter-hemispheric connections over the motor regions, as well as the connections linking the occipital (visual) and frontal areas. This hypothesised outcome was indeed observed, as depicted by the red lines in Fig. 2H.

We used histograms of correlation coefficients as a guide in discovering connectivity related to learning (Fig. 3). This is a conservative approach, since a histogram will deviate from the null distribution only if there is a pervasive pattern of correlations with the same sign outweighing those of the opposite sign; strong individual correlations potentially due to chance are not sufficient to skew the histogram (Figures S2-S5).

During initial rest, many of the frontal and central but also occipital connections in the delta range positively correlated with subsequent improvements in performance. Therefore the rightward skew in the 3 Hz histogram in Fig. 3A implied that pre-task connectivity in the delta band was important for learning. Figure 3C shows only 3 Hz connections but the neighbouring frequencies displayed a similar pattern. Investigating the extent to which *changes* in connectivity correlate with learning (Figure S7) showed that high learners had significantly greater task-evoked declines in delta band connectivity (Figure S7B).

Studies of the association between delta connectivity and motor behaviour are scarce and no study, to our knowledge, reports on the link between delta power and learning laparoscopy tasks. In a study of video game learning, delta EEG power positively correlated with improvements in cognitive control[43]. However in other studies involving simple motor tasks, there was negative[44] or no correlation[45] between learning and pre-task, resting delta power. Thus our findings about the predictive role of resting and task-evoked changes in delta connectivity for fast motor learning warrants further study.

Figure 2 showed that task execution was linked to a decrease in frontoparietal alpha as well as an increase in occipitofrontal high beta connections. These networks were absent from Fig. 3 since the associated histograms of the correlation coefficients remained within the confidence intervals. However by closely examining the correlations between ISPC with RSI, we have found that inter-subject differences in these networks during the pre-task rest episode were in fact predictive of better learning (Figure S2E and H, respectively). Thus the networks during rest which correlate with RSI share some commonalities with the task activated ones; notably, participants with greater alpha desynchronisation of the DMN and high-beta synchronisation of occipital-frontal networks were shown to be better future fast learners.

Figure 3F indicates that better learners had greater suppression of their beta band brain communications during training tasks. This may be related to plasticity-inducing effects of movement related beta desynchronisation[46]. The pivotal appearance of frontopolar and frontoparietal sites in our results may reflect the fact that beta oscillations code for feedback in reward related structures such as orbitofrontal cortex and covary with BOLD in cortico-basal ganglia-thalamic circuitry[47,48]. Beta desynchronisation in frontal and sensorimotor areas has been linked to implementing corrective movements and faster learning from performance feedback[49–51].

A recent study suggests that early motor skill is acquired through reinforcement learning in basal ganglia under cortical supervision, while slower associative learning between basal ganglia and the thalamus accounts for skill automation[23]. Basal ganglia and the sensorimotor cortex are the two principal sources of beta oscillations[46]. These suggest that the beta connections in Fig. 3F interlinking prefrontal, frontoparietal, and occipitofrontal areas are promising candidates as neural markers for the extent of fast learning in laparoscopy training.

BDNF expression in cortical neurons that project to basal ganglia is essential for motor learning[52]. We observed a steady decline in group averaged BDNF expression during the course of the training session (Table S4), presumably reflecting a decrease in the need for BDNF-facilitated neural plasticity. We also observed an association between higher BDNF levels and lower connectivity centred on the left temporal areas, revealed by connections with electrode T7 observed in Fig. 4F across multiple frequencies. In addition, beta connectivity between left temporal and frontal and central areas were lower during the repeat task and second task relative to initial task performance (Figure S4).

Previous studies have determined that verbal-analytical processes diminish with increasing motor proficiency[53–55]. Our findings support the neural efficiency hypothesis whereby conscious, verbal-analytical functionality may interfere with the implicit learning needed for acquiring many motor skills[56]. However we did not find any correlations between BDNF and RSI (Table S3), which suggests that BDNF may be primarily a facilitator of slow learning.

Figure 5A, C show task execution simultaneously led to greater network integration (lower λ) as well as greater segregation (higher CC) above 16 Hz, bringing the functional networks closer to small-world architectures. This was an expected consequence of the task-evoked increases in ISPC above 16 Hz across all cortical distances studied in Fig. 2A-E. The plots of λ and CC had local alpha peaks (Fig. 5A, C) while the plots of r_{λ} and r_{CC} had local delta peaks (Fig. 5B, D), indicating that alpha connectivity, although strongly affected by task performance, was not strongly linked with learning.

It was shown in a previous study that greater network segregation at rest across all bands promotes learning[44] whereas we found this to be the case only for the delta range. Furthermore we found that network integration and segregation depended strongly on the frequency of the underlying functional connections. Yet for any given frequency, the task-related shifts in integration were similar to the shifts in segregation. This implied that task performance affected connectivity at different cortical distances in similar ways, since λ is influenced primarily by long distance and CC by short distance connections.

The limitations of this study include the following: (1) We did not measure participants' baseline visuospatial ability, video game experience and other characteristics known to affect the performance of laparoscopy learners[37,57,58] that could have helped explain the observed distribution of baseline performance. (2) We only studied episode-averaged ISPC whereas intra-episode variability of functional connectivity may carry additional useful information relevant to motor learning[59]. (3) Phase difference between pairs of signals can be investigated as an additional metric. (4) Gender-specific patterns in our data should be investigated which this paper has not done. (5) We have only used 19 electrodes and calculated sensor level functional connectivity whereas a higher density coverage of electrodes on the scalp allowing the extraction of source activity, particularly in subcortical structures which are key parts of motor learning, can be tracked[60].

Conclusions

Our findings shed light on the functional connectivity changes underpinning motor skill acquisition in laparoscopy training. We hope that our work paves the way for more effective interventions to augment motor learning across a range of applications. Potential applications include the development of neurofeedback systems that utilise connectivity[13,50,61] as well as brain stimulation approaches[31,62]. While our study focused specifically on laparoscopic skills, understanding the neural basis of motor learning has implications for diverse domains including sports[63], music performance[64], inclusive ergonomic design[65], and rehabilitation[66].

Materials and methods

The experimental design and data collection were described in our previous publications[6,67]. In this section, while summarising the experiments we focus on the methodology specifically relevant to the results in the present paper.

Participants

A total of 38 healthy adult volunteers without prior experience in laparoscopic surgery participated in a trial to perform predetermined basic laparoscopic tasks on a laparoscopic simulator. One participant could not enroll due to their hairstyle, which made it impossible to fit the cap and record EEG data. Technical problems prohibited the recording of data for four participants. Two participants were excluded from the analysis due to issues with the time stamps routine. Hence the final sample consisted of 31 participants (17 females, 14 males) with a mean age of 21.61 ± 2.12 years. All participants provided written informed consent prior to the study and received gift vouchers for their participation. The study was approved by the Ethical Committee of the College of Science and Technology at the Nottingham Trent University and all methods were performed in accordance with the relevant guidelines and regulations. Informed consent was obtained from all subjects and/or their legal guardian(s) for publication of identifying information/images in an online open-access publication.

Experimental design

The experiment was conducted in a training laboratory equipped with a Laparoscopic Surgery (LS) trainer box by Inovus Surgical Solutions (The Pyxus laparoscopic box trainer by Inovus Medical—43 cm × 33 cm × 31 cm) and a 21-inch monitor. Each trial lasted approximately an hour, including the time spent to set up the system and devices and perform the tasks. At the beginning of the trial, participants received instructions about the session via a training video, followed by a hands-on introduction to help them become competent before commencing the training. The LS trainer box was equipped with a centrally mounted camera and a light source, with the entry ports of the instruments separated by 13.5 cm. The training bases (14 cm × 10 cm) were placed in the LS trainer

box and centred in the camera's field of view. Laparoscopic video was projected onto the monitor, which was in the direct view of the participant.

Training tasks

To perform the primary tasks participants stood in front of the LS trainer box during the performance of Laparoscopic and secondary tasks (Fig. 1A). The laparoscopic tasks completion time was recorded, with a maximum time of 15 min. The Ring Transfer task involved grasping, lifting, and relocating rings from one rod to another using both surgical instruments. Four rods (A, B, C, and D) were arranged on a ring stack base. Participants used their left-hand to transfer rings from rod A to B, then passed each ring from B to C using the left-hand and right-hand, and finally moved the rings from C to D using the right-hand only. The Threading task consisted of passing a piece of string through holes labelled 1–7 on a Threading base. Participants could use both surgical tools and both hands. To simulate potential distractions or disruptions (e.g., auditory alarms) that may arise in a realistic setting, an auditory task was added to the experiment. Participants had to respond to a series of beeps as quickly as possible by pressing down on a foot pedal.

Experimental procedure and data collection. The experiment started by having the participants perform the secondary task alone for two minutes. For the rest of the experiment, participants performed primary and secondary tasks simultaneously. The primary tasks included two Fundamentals of Laparoscopic Surgery tasks, Ring Transfer and Threading, in alternating sequence (T1 and T2) followed by a repetition of the first task (T1R). Fingertip blood samples were taken at baseline (before T0) and immediately after the completion of each task to determine the serum cortisol and brain-derived neurotropic factor (BDNF) concentrations. Cortisol data[67] were not used in the current paper. The participants filled in the NASA-TLX questionnaire after each task. A rest period of 2 min was taken after the initial secondary task performed alone and after each blood sample, prior to performing the next task (Fig. 1B).

Analysis of motor learning

To quantify fast motor learning we calculated the Rescaled Speed Increment (RSI) for each participant, by comparing the completion times (CT) of the initial and repeat performances of the same task. After calculating the task completion speed as the inverse of the completion time, $S = 1/CT$ (in units of minutes per task), we determined the speed increment, $\Delta S = S_{T1R} - S_{T1}$ as the speed in the repeated minus that in the initial performance. However ΔS strongly depended on the initial performance (speed in T1), as clearly inferred from Fig. 1C. Therefore to construct an indicator of motor learning independent of the participants' baseline performance, we normalised the speed increment by the initial speed to obtain $RSI = \Delta S/S_{T1}$. The rescaled speed increment can be algebraically recast in the form $RSI = C_{T1}/C_{T1R} - 1$, which has a natural interpretation. RSI measures the extent to which the ratio CT1/CT1R is greater than unity, such that if CT1R = CT1 then RSI = 0 (no learning), and if $C_{T1R} < C_{T1}$ then $RSI > 0$. Thus positive values of RSI signify the extent of motor learning. To establish the occurrence of learning in motor tasks it is important to control for changes in accuracy[33]. This was done by using the overall error rate calculated as the average of the rates of two types of error: (i) dropping a ring on the stack board and (ii) dropping it outside the board.

EEG pre-processing

The raw EEG data underwent a series of pre-processing steps to remove non-brain signals and preserve the brain signal for further analysis. Segments of data containing high-frequency, high-amplitude waves, likely originating from gross body movements during EEG recording, were identified and deleted using a 1 s wide sliding window. Additionally, electrodes exhibiting kurtosis values exceeding 5 were considered invalid channels and removed from the data. The signals were then band-pass filtered between 0.16 Hz and 40 Hz to reduce slow drifts and high-frequency artifacts, and subsequently down sampled to 200 Hz to optimise computational and storage requirements. To segregate components such as eye blinks and movements, Independent Component Analysis (ICA) decomposition using the Extended-Infomax algorithm was applied to the filtered EEG data. The ADJUST method was then used to automatically detect and remove independent components associated with artifacts, and the power spectrum, time series, and topographic maps of the independent components were visually inspected to further refine the artifact removal process. Finally, the pre-processed data, with the artifact components removed, was reconstructed for further analysis.

Functional connectivity

We calculated the Inter-Site Phase-Clustering (ISPC), also known as Phase Locking Value (PLV), for each unordered pair of electrodes within 1 Hz wide frequency bands centred at 1 Hz, 2 Hz, …, 40 Hz. ISPC was used to represent the strength of the functional connection between pairs of sites[30,34,68]. For each value of ISPC the associated cortical distance was computed based on the MNI coordinates of the main neuronal populations associated with each electrode[35]. Narrow-band analysis was used to avoid potential loss of information from pooling variables into the traditional, wider frequency bands and to generate more reliable phase estimates[69]. To minimise possible distortions of the ISPC by volume conduction we used the Laplace montage that subtracted from the instantaneous signal the mean of its nearest neighbours[70]. Alternative methods insensitive to volume conduction (e.g. weighted phase lag index[71] were not used, as modelling and experiment suggest zero-lag synchronisation can occur in the presence of conduction delays[72–74] and play a key role in visuomotor performance (Roelfsema et al., 1997). We selected ISPC as phase coupling has high intra-subject test-retest reliability[75] and it emphasises synchrony based only on phase whereas coherence, a widely used alternative measure of connectivity, weights individual phase angles by band-power[34].

In addition, we sought to quantify overall connectivity with a small number of neurobiologically meaningful and easily computable measures with the help of graph theory. For each frequency band, an undirected graph

was constructed with electrodes representing the nodes and the weight of the edges given by the ISPC. We used weighted functional connections (rather than binary connections), as thresholding could eliminate potentially valuable information[76,77]. We next determined the clustering coefficient (CC) and characteristic path length (λ), which are commonly used in network analysis. CC measures how well connected the neighbours of a typical node are to one another, and high values of CC are associated with functional segregation. λ is the mean shortest path over all pairs of nodes, where the distance was calculated from the inverse of ISPC values. It quantifies the capacity for information transfer across the network, and low values of λ are associated with greater functional integration. We investigated potential association of ISPC, CC and λ with motor learning by determining the Pearson correlation of the relevant quantity.

Statistical analysis

In assessing the significance of the difference between two sets of related values, the Wilcoxon Signed-Rank test was used for paired data, and the Kolmogorov-Smirnov (KS) test for unpaired values. Null distributions and the related 95% confidence intervals for the correlation coefficients (e.g. Fig. 3A,E) were constructed by recalculating the coefficients repeatedly 1000 times after randomly shuffling the order of participants' RSI values. In calculating the statistical significance of the difference in connectivity between distinct episodes (e.g. Task and Rest) we calculated, for each connection (i.e. electrode pair) the p-value of the difference using the paired Wilcoxon Singed-Rank test. Given 6 frequency bands and $n = 19$ EEG channels, a total of $6n(n-1)/2 = 1026$ distinct ISPC values were calculated for each experimental condition. In multiple comparisons of connectivity measures across all electrode pairs, the false discovery rate (FDR) was controlled using the Benjamini-Hochberg approach[78].

Data availability

The data and computer programs underlying the study are publicly accessible at https://doi.org/10.5281/zenodo.12810004. Researchers interested in accessing underlying samples for further analysis will be able to contact the corresponding author to discuss the process for obtaining an MTA.

Received: 24 August 2024; Accepted: 4 February 2025
Published online: 03 March 2025

References

1. Gandolfo, F., Mussa-Ivaldi, F. A. & Bizzi, E. Motor learning by field approximation. *Proc. Natl. Acad. Sci.* **93**, 3843–3846 (1996).
2. White, A. D. et al. Laparoscopic motor learning and workspace exploration. *J. Surg. Educ.* **73**, 992–998 (2016).
3. Carswell, C. M., Clarke, D. & Seales, W. B. assessing mental workload during laparoscopic surgery. *Surg. Innov.* **12**, 80–90 (2005).
4. Hannah, T. C. et al. Neuromonitoring correlates of Expertise Level in Surgical performers: a systematic review. *Front. Hum. Neurosci.* **16**, (2022).
5. Nemani, A. et al. Assessing bimanual motor skills with optical neuroimaging. *Sci. Adv.* **4**, eaat3807 (2018).
6. Zakeri, Z., Mansfield, N., Sunderland, C. & Omurtag, A. Physiological correlates of cognitive load in laparoscopic surgery. *Sci. Rep.* **10**, 1–13 (2020).
7. Boettcher, M. et al. The spaced learning concept significantly improves training for laparoscopic suturing: a pilot randomized controlled study. *Surg. Endosc.* **32**, 154–159 (2018).
8. El Boghdady, M. & Alijani, A. Feedback in surgical education. *Surgeon* **15**, 98–103 (2017).
9. Gallagher, A. G., Jordan-Black, J. A. & O'Sullivan, G. C. Prospective, randomized assessment of the acquisition, maintenance, and loss of laparoscopic skills. *Ann. Surg.* **256**, 387–393 (2012).
10. Sigrist, R., Rauter, G., Riener, R. & Wolf, P. Augmented visual, auditory, haptic, and multimodal feedback in motor learning: A review. *Psychonom. Bull. Rev.* **20**. https://doi.org/10.3758/s13423-012-0333-8 (2013).
11. Spruit, E. N., Band, G. P. H., Hamming, J. F. & Ridderinkhof, K. R. Optimal training design for procedural motor skills: A review and application to laparoscopic surgery. *Psychol. Res.* **78**. https://doi.org/10.1007/s00426-013-0525-5 (2014).
12. Lebares, C. C. et al. Efficacy of mindfulness-based cognitive training in surgery additional analysis of the mindful surgeon pilot randomized clinical trial. *JAMA Netw. Open.* **2** (2019).
13. Li, G., Li, H., Pu, J., Wan, F. & Hu, Y. Effect of brain alpha oscillation on the performance in laparoscopic skills simulator training. *Surg. Endosc.* **35**, 584–592 (2021).
14. Fitts, P. M. & Peterson, J. R. Information capacity of discrete motor responses. *J. Exp. Psychol.* **67**, 103 (1964).
15. Seidler, R. D., Kwak, Y., Fling, B. W. & Bernard, J. A. Neurocognitive mechanisms of Error-Based Motor Learning. in Progress in Motor Control (eds Richardson, M. J., Riley, M. A. & Shockley, K.) vol. 782 39–60 (Springer New York, New York, NY, (2013).
16. Karni, A. & Sagi, D. The time course of learning a visual skill. *Nature* **365**, 250–252 (1993).
17. Doyon, J. et al. Contributions of the basal ganglia and functionally related brain structures to motor learning. *Behav. Brain. Res.* **199**, 61–75 (2009).
18. Immink, M. A., Verwey, W. B. & Wright, D. L. In *The Neural Basis of Cognitive Efficiency in Motor Skill Performance from Early Learning to Automatic Stages*. 221–249 (eds Neuroergonomics, C. S.) (Springer International Publishing, 2020). https://doi.org/10.1007/978-3-030-34784-0_12.
19. Kumar, N., Sidarta, A., Smith, C. & Ostry, D. J. Ventrolateral prefrontal cortex contributes to human motor learning. eNeuro 9, (2022).
20. Halsband, U. & Lange, R. K. Motor learning in man: a review of functional and clinical studies. *J. Physiology-Paris.* **99**, 414–424 (2006).
21. Poldrack, R. A. et al. The neural correlates of motor skill automaticity. *J. Neurosci.* **25**, 5356–5364 (2005).
22. Wolff, S. B. E., Ko, R. & Ölveczky, B. P. Distinct roles for motor cortical and thalamic inputs to striatum during motor skill learning and execution. *Sci. Adv.* **8**, eabk0231 (2022).
23. Murray, J. M. & Escola, G. S. Remembrance of things practiced with fast and slow learning in cortical and subcortical pathways. *Nat. Commun.* **11**, 6441 (2020).
24. Sun, F. T., Miller, L. M., Rao, A. A. & D'Esposito, M. Functional connectivity of cortical networks involved in bimanual motor sequence learning. *Cereb. Cortex.* **17**, 1227–1234 (2007).
25. Yu, M., Song, H., Huang, J., Song, Y. & Liu, J. Motor learning improves the stability of large-scale brain connectivity pattern. *Front. Hum. Neurosci.* **14**, 571733 (2020).

26. Engel, A. K., Gerloff, C., Hilgetag, C. C. & Nolte, G. Intrinsic coupling modes: multiscale interactions in ongoing brain activity. *Neuron* **80**, 867–886 (2013).
27. Uhlhaas, P. et al. Neural synchrony in cortical networks: history, concept and current status. *Front. Integr. Neurosci.* **3**, 543 (2009).
28. Ward, L. M. Synchronous neural oscillations and cognitive processes. *Trends Cogn. Sci.* **7**, 553–559 (2003).
29. Dragomir, A. & Omurtag, A. Brain's Networks and Their Functional Significance in Cognition. in Handbook of Neuroengineering (ed. Thakor, N. V) 1–30 (Springer, Singapore, 2020). https://doi.org/10.1007/978-981-15-2848-4_76-2.
30. Lachaux, J. P., Rodriguez, E., Martinerie, J. & Varela, F. J. Measuring phase synchrony in brain signals. *Hum. Brain Mapp.* **8**, 194–208 (1999).
31. Reis, J. et al. Noninvasive cortical stimulation enhances motor skill acquisition over multiple days through an effect on consolidation. *Proc. Natl. Acad. Sci.* **106**, 1590–1595 (2009).
32. Hiramoto, R. et al. BDNF as a possible modulator of EEG oscillatory response at the parietal cortex during visuo-tactile integration processes using a rubber hand. *Neurosci. Res.* **124**, 16–24 (2017).
33. Fitts, P. M. & Posner M. I. Human performance. (1967).
34. Cohen, M. X. *Analyzing Neural Time Series Data: Theory and Practice* (MIT Press, 2014).
35. Scrivener, C. L. & Reader, A. T. Variability of EEG electrode positions and their underlying brain regions: visualizing gel artifacts from a simultaneous EEG-fMRI dataset. *Brain Behav.* **12**, (2022).
36. Keles, H. O., Cengiz, C., Demiral, I., Ozmen, M. M. & Omurtag, A. High density optical neuroimaging predicts surgeons's subjective experience and skill levels. *PLoS One*. **16**, e0247117 (2021).
37. Keles, H. O. & Omurtag, A. Video game experience affects performance, cognitive load, and brain activity in laparoscopic surgery training. (2021).
38. Makino, H., Hwang, E. J., Hedrick, N. G. & Komiyama, T. Circuit mechanisms of sensorimotor learning. *Neuron* **92**, 705–721 (2016).
39. Peters, A. J., Chen, S. X. & Komiyama, T. Emergence of reproducible spatiotemporal activity during motor learning. *Nature* **510**, 263–267 (2014).
40. Rosen, B. Q. & Halgren, E. An estimation of the absolute number of axons indicates that human cortical areas are sparsely connected. *PLoS Biol.* **20**, e3001575 (2022).
41. Buzsaki, G., Logothetis, N. & Singer, W. Scaling brain size, keeping timing: evolutionary preservation of brain rhythms. *Neuron* **80**, 751–764 (2013).
42. Clancy, K. J. et al. Transcranial stimulation of alpha oscillations up-regulates the default mode network. *Proc. Natl. Acad. Sci.* **119**, e2110868119 (2022).
43. Mathewson, K. E. et al. Different slopes for different folks: alpha and delta span style=font-variant:small-caps;EEG/span power predict subsequent video game learning rate and improvements in cognitive control tasks. *Psychophysiology* **49**, 1558–1570 (2012).
44. Titone, S. et al. Connectivity in large-scale resting-state Brain Networks is related to Motor Learning: a high-density EEG study. *Brain Sci.* **12**, (2022).
45. Ozdenizci, O. et al. Electroencephalographic identifiers of motor adaptation learning. *J. Neural Eng.* **14**, 46027 (2017).
46. Brittain, J. S. & Brown, P. Oscillations and the basal ganglia: motor control and beyond. *Neuroimage* **85**, 637–647 (2014).
47. Marco-Pallares, J. et al. Human oscillatory activity associated to reward processing in a gambling task. *Neuropsychologia* **46**, 241–248 (2008).
48. Matsumoto, M., Matsumoto, K., Abe, H. & Tanaka, K. Medial prefrontal cell activity signaling prediction errors of action values. *Nat. Neurosci.* **10**, 647–656 (2007).
49. Basanisi, R., Marche, K., Combrisson, E., Apicella, P. & Brovelli, A. Beta oscillations in monkey striatum encode reward prediction error signals. *J. Neurosci.* **43**, 3339–3352 (2023).
50. Luft, C. D. B. Learning from feedback: the neural mechanisms of feedback processing facilitating better performance. *Behav. Brain. Res.* **261**, 356–368 (2014).
51. Van Vugt, F. T., Near, J., Hennessy, T., Doyon, J. & Ostry, D. J. Early stages of sensorimotor map acquisition: neurochemical signature in primary motor cortex and its relation to functional connectivity. *J. Neurophysiol.* **124**, 1615–1624 (2020).
52. Andreska, T. et al. Induction of BDNF expression in layer II/III and layer V neurons of the motor cortex is essential for motor learning. *J. Neurosci.* **40**, 6289–6308 (2020).
53. Deeny, S. P., Hillman, C. H., Janelle, C. M. & Hatfield, B. D. Cortico-cortical communication and superior performance in skilled marksmen: an EEG coherence analysis. *J. Sport Exerc. Psychol.* **25**, (2003).
54. Percio, C. et al. Movement-related desynchronization of alpha rhythms is lower in athletes than non-athletes: a high-resolution EEG study. *Clin. Neurophysiol.* **121**, (2010).
55. Parr, J. V. V., Vine, S. J., Wilson, M. R., Harrison, N. R. & Wood, G. Visual attention, EEG alpha power and T7-Fz connectivity are implicated in prosthetic hand control and can be optimized through gaze training. *J. Neuroeng. Rehabil.* **16**, 52 (2019).
56. Zhu, F. F. et al. Implicit motor learning promotes neural efficiency during laparoscopy. *Surg. Endosc.* **25**, 2950–2955 (2011).
57. Beattie, K. L., Hill, A., Horswill, M. S., Grove, P. M. & Stevenson, A. R. L. Aptitude and attitude: predictors of performance during and after basic laparoscopic skills training. *Surg. Endosc.* **36**, 3467–3479 (2022).
58. Harrington, C. M., Dicker, P., Traynor, O. & Kavanagh, D. O. Visuospatial abilities and fine motor experiences influence acquisition and maintenance of fundamentals of laparoscopic surgery (FLS) task performance. *Surg. Endosc.* **32**, 4639–4648 (2018).
59. Seedat, Z. A. et al. The role of transient spectral 'bursts' in functional connectivity: a magnetoencephalography study. *Neuroimage* **209**, (2020).
60. Cebolla, A. M., Palmero-Soler, E., Leroy, A. & Cheron, G. EEG spectral generators involved in motor imagery: a swLORETA study. *Front. Psychol.* **8**, 284479 (2017).
61. Modi, H. et al. A Decade of Imaging Surgeons' Brain Function (part I): Terminology, Techniques, and Clinical Translation. Elsevier.
62. Wessel, M. J. et al. Noninvasive theta-burst stimulation of the human striatum enhances striatal activity and motor skill learning. *Nat. Neurosci.* **26**, 2005–2016 (2023).
63. Yarrow, K., Brown, P. & Krakauer, J. W. Inside the brain of an elite athlete: the neural processes that support high achievement in sports. *Nat. Rev. Neurosci.* **10**, 585–596 (2009).
64. Cantou, P., Platel, H., Desgranges, B. & Groussard, M. How motor, cognitive and musical expertise shapes the brain: Focus on fMRI and EEG resting-state functional connectivity. *J. Chem. Neuroanat.* **89**. https://doi.org/10.1016/j.jchemneu.2017.08.003 (2018).
65. Durand-Ruel, M. et al. Early motor skill acquisition in healthy older adults: brain correlates of the learning process. *Cereb. Cortex* **33**, (2023).
66. Dahms, C., Brodoehl, S., Witte, O. W. & Klingner, C. M. The importance of different learning stages for motor sequence learning after stroke. *Hum. Brain Mapp.* **41**, 270–286 (2020).
67. Zakeri, Z., Mansfield, N., Sunderland, C. & Omurtag, A. Cross-validating models of continuous data from simulation and experiment by using linear regression and artificial neural networks. *Inf. Med. Unlocked*. **21**, 100457 (2020).
68. Omurtag, A., Aghajani, H. & Keles, H. O. Decoding human mental states by whole-head EEG + fNIRS during category fluency task performance. *J. Neural Eng.* **14**, 66003 (2017).
69. Dvorak, D. & Fenton, A. A. Toward a proper estimation of phase–amplitude coupling in neural oscillations. *J. Neurosci. Methods.* **225**, 42–56 (2014).

70. Kayser, J. & Tenke, C. E. On the benefits of using surface Laplacian (current source density) methodology in electrophysiology. *Int. J. Psychophysiol.* **97**, 171 (2015).
71. Vinck, M., Oostenveld, R., Van Wingerden, M., Battaglia, F. & Pennartz, C. M. A. An improved index of phase-synchronization for electrophysiological data in the presence of volume-conduction, noise and sample-size bias. *Neuroimage* **55**, 1548–1565 (2011).
72. Fischer, I. et al. Zero-lag long-range synchronization via Dynamical Relaying. *Phys. Rev. Lett.* **97**, 123902 (2006).
73. Sirovich, L., Omurtag, A. & Lubliner, K. Dynamics of neural populations: Stability and synchrony. *Network: Comput. Neural Syst.* **17**, 3–29 (2006).
74. Viriyopase, A., Bojak, I., Zeitler, M. & Gielen, S. When long-range zero-lag synchronization is feasible in cortical networks. *Front. Comput. Neurosci.* **6**, 49 (2012).
75. Nentwich, M. et al. Functional connectivity of EEG is subject-specific, associated with phenotype, and different from fMRI. *Neuroimage* **218**, 117001 (2020).
76. Bassett, D. S. & Bullmore, E. T. Small-world brain networks revisited. *Neuroscientist* **23**, 499–516 (2017).
77. Bolanos, M., Bernat, E. M., He, B. & Aviyente, S. A weighted small world network measure for assessing functional connectivity. *J. Neurosci. Methods*. **212**, 133–142 (2013).
78. Benjamini, Y. & Hochberg, Y. Controlling the false discovery rate: a practical and powerful approach to multiple testing. *J. Roy. Stat. Soc.: Ser. B (Methodol.)*. **57**, 289–300 (1995).

Acknowledgements

This research was made possible in part by support from the Foundation for Neurofeedback and Neuromodulation Research (602–2023) provided to A.O.

Author contributions

A.O. designed the study, performed the analysis, and wrote the manuscript. N.M. and C.S. designed the study, supervised the research work. Z.Z. designed the study, performed the experiments and analysis. All authors reviewed and edited the manuscript.

Declarations

Competing interests

The authors declare no competing interests.

Additional information

Supplementary Information The online version contains supplementary material available at https://doi.org/10.1038/s41598-025-89261-0.

Correspondence and requests for materials should be addressed to A.O.

Reprints and permissions information is available at www.nature.com/reprints.

Publisher's note Springer Nature remains neutral with regard to jurisdictional claims in published maps and institutional affiliations.